Cancer Research

Angiopoietin-2 Regulates Gene Expression in TIE2-Expressing Monocytes and Augments Their Inherent Proangiogenic Functions

Seth B. Coffelt[1], Andrea O. Tal[3], Alexander Scholz[3], Michele De Palma[5], Sunil Patel[1], Carmen Urbich[4], Subhra K. Biswas[6], Craig Murdoch[2], Karl H. Plate[3], Yvonne Reiss[3], and Claire E. Lewis[1]

Abstract

TIE2-expressing monocytes/macrophages (TEM) are a highly proangiogenic subset of myeloid cells in tumors. Here, we show that circulating human TEMs are already preprogrammed in the circulation to be more angiogenic and express higher levels of such proangiogenic genes as matrix metalloproteinase-9 (*MMP-9*), *VEGFA, COX-2*, and *WNT5A* than TIE2$^-$ monocytes. Additionally, angiopoietin-2 (ANG-2) markedly enhanced the proangiogenic activity of TEMs and increased their expression of two proangiogenic enzymes: thymidine phosphorylase (*TP*) and cathepsin B (*CTSB*). Three "alternatively activated" (or M2-like) macrophage markers were also upregulated by ANG-2 in TEMs: *interleukin-10*, mannose receptor (*MRC1*), and *CCL17*. To investigate the effects of ANG-2 on the phenotype and function of TEMs in tumors, we used a double-transgenic (DT) mouse model in which ANG-2 was specifically overexpressed by endothelial cells. Syngeneic tumors grown in these ANG-2 DT mice were more vascularized and contained greater numbers of TEMs than those in wild-type (WT) mice. In both tumor types, expression of MMP-9 and MRC1 was mainly restricted to tumor TEMs rather than TIE2$^-$ macrophages. Furthermore, tumor TEMs expressed higher levels of MRC1, TP, and CTSB in ANG-2 DT tumors than WT tumors. Taken together, our data show that although circulating TEMs are innately proangiogenic, exposure to tumor-derived ANG-2 stimulates these cells to exhibit a broader, tumor-promoting phenotype. As such, the ANG-2–TEM axis may represent a new target for antiangiogenic cancer therapies. *Cancer Res; 70(13); 5270–80. ©2010 AACR.*

Introduction

TIE2-expressing monocytes/macrophages (TEMs) are a subpopulation of circulating and tumor-infiltrating myeloid cells with profound proangiogenic activity, found in both humans and mice (1–4). TEM ablation studies in mice have shown that this subpopulation plays a greater role in regulating tumor angiogenesis than TIE2$^-$ tumor-associated macrophages (TAM; refs. 1, 5). Similarly, when circulating TEMs are coinjected with Matrigel in mice, microvessel density (MVD) is higher than that seen with TIE2$^-$ monocytes, suggesting that they possess an inherent ability to stimulate angiogenesis (1, 4). Various phenotypic differences have emerged recently between TEMs and TIE2$^-$ TAMs in murine tumors, with TEMs exhibiting various markers of an alternatively activated (i.e., M2-like) phenotype (5).

Angiopoietins are a family of molecules known to bind to, and activate, the TIE2 receptor on endothelial cells (EC; refs. 6–9). Angiopoietins play an essential role in regulating angiogenesis and vascular homeostasis. Angiopoietin-1 (ANG-1) maintains the integrity of the endothelium, whereas angiopoietin-2 (ANG-2) was thought until recently to act as an ANG-1 antagonist to destabilize the vasculature (10). However, it now seems that the exact influence of ANG-2 on endothelium is highly dependent on the local cytokine milieu. Together with other cytokines such as vascular endothelial growth factor (VEGF), ANG-2 stimulates angiogenic responses, but without such cofactors, it elicits vessel regression (7, 11, 12). During inflammation, ANG-2 also sensitizes the endothelium to tumor necrosis factor α (TNFα), and together, they regulate expression of adhesion molecules and leukocyte adherence (13).

Authors' Affiliations: [1]Academic Unit of Inflammation and Tumour Targeting, University of Sheffield Medical School; [2]Department of Oral and Maxillofacial Medicine and Surgery, University of Sheffield School of Clinical Dentistry, Sheffield, United Kingdom; [3]Institute of Neurology/Edinger Institute, Frankfurt University Medical School; [4]Institute for Cardiovascular Regeneration, Centre of Molecular Medicine Goethe-University, Frankfurt, Germany; [5]Angiogenesis and Tumor Targeting Research Unit, Division of Regenerative Medicine, Stem Cells and Gene Therapy, San Raffaele Scientific Institute, Milan, Italy; and [6]Singapore Immunology Network, Biomedical Sciences Institutes, Agency for Science, Technology and Research, Singapore, Singapore

Note: Supplementary data for this article are available at Cancer Research Online (http://cancerres.aacrjournals.org/).

S.B. Coffelt and A.O. Tal contributed equally to this work as co-first authors and K.H. Plate, Y. Reiss, and C.E. Lewis contributed equally to this work as co-senior authors.

Corresponding Author: Claire E. Lewis, Academic Unit of Inflammation and Tumour Targeting, University of Sheffield Medical School, Sheffield S10 2RX, United Kingdom. Phone: 44-114-271-2903; Fax: 44-114-271-2903; E-mail: claire.lewis@sheffield.ac.uk.

doi: 10.1158/0008-5472.CAN-10-0012

In human tumors, the ANG-1/ANG-2 balance is often skewed in favor of ANG-2 and vascular remodeling. ANG-2 overexpression has been shown in several tumor types (14–19), where it is produced by the endothelium and occasionally by tumor cells (14, 20). ANG-2 has a complex and sometimes contradictory role during tumor progression. For example, ANG-2 overexpression by tumor xenografts leads to advanced proliferation, increased angiogenesis, and enhanced invasiveness (11, 14–16, 21–23), but it delays tumor growth and disrupts angiogenesis in other tumor types (24, 25). Syngeneic tumors grown in *Ang-2* knockout mice show slower proliferation during the initial stages of tumor progression, decreased vessel diameter, and increased pericyte vessel coverage (26).

We recently reported that ANG-2 modulates the secretion of certain inflammatory cytokines by human monocytes *in vitro* (3, 4). However, information about the role of ANG-2 in regulating the tumor-promoting functions of TEMs is lacking. We therefore examined the influence of ANG-2 on expression of various tumor-promoting genes by human circulating TEMs *in vitro* and murine tumor-infiltrating TEMs *in vivo*.

Materials and Methods

Monocyte isolation and culture

Monocytes were isolated as previously described (3, 27). Pacific blue–conjugated anti-CD14 (1:20 per 10^6 cells; clone M5E2; BD Biosciences) and allophycocyanin (APC)–conjugated anti-TIE2 (1:10 per 10^6 cells; clone 83715; R&D Systems) antibodies were used to identify TEMs. Monocytes were sorted into cold Iscove's modified Dulbecco's medium (IMDM; BioWhittaker) containing 2% fetal bovine serum (FBS) and 2 mmol/L L-glutamine (Sigma-Aldrich) using a FACSAria II flow cytometer (BD Biosciences). Typically, 2×10^6 cells were collected from each sort with a purity of ~90%. When required, 10^6 cells were seeded onto plastic with IMDM–2% FBS and then placed into a humidified 37°C incubator with 5% CO_2.

Quantitative real-time PCR

Total RNA was extracted from monocytes using RNeasy kit (Qiagen). RNA from 10^6 cells was isolated immediately following fluorescence-activated cell sorting (FACS). For experiments involving ANG-1/ANG-2 treatment, sorted populations were cultured overnight, washed the next day, and then exposed to 300 ng/mL of recombinant angiopoietins (R&D Systems) for 6 hours. RNA (250–500 ng) was reverse transcribed using Precision RT kit (PrimerDesign). cDNA was amplified with Taqman master mix (Applied Biosystems) or Precision Mastermix (PrimerDesign) containing SYBR Green. PCR cycling conditions were as described using ABI 7900HT Sequence Detection System (Applied Biosystems; ref. 27). Samples were run on the same plate as the housekeeping gene [tyrosine 3-monooxygenase/tryptophan 5-monooxygenase activation protein (YWHAZ1) for SYBR Green probes, and β2-microglobulin for Taqman probes] in triplicate. Experiments were performed four to six times. Differences in gene expression were determined by the quantitative comparative C_t (threshold value) method.

Soluble protein analysis

Conditioned medium was collected from sorted monocyte subsets after 24 hours in culture. VEGF, interleukin (IL)-6, and IL-10 were quantified by cytometric bead array using a FACSArray bioanalyzer (BD Biosciences). Epidermal growth factor (EGF) levels were measured by ELISA (PreproTech). Matrix metalloproteinase-9 (MMP-9) activity was assessed by zymography in which proteins were separated in 10% SDS-polyacrylamide gels containing 0.1% gelatin. Following incubation in developing buffer, the gels were washed in distilled water and then stained with SimplyBlue SafeStain (Invitrogen). Quantification of band intensity was performed by using ImageJ software (NIH, Bethesda, MD). Human ANG-2 (hANG-2) blood serum levels in mice were detected by ELISA (R&D Systems) after 1:2 dilution. All other soluble factors were analyzed with Bio-Plex Cytokine Assays (Bio-Rad).

In vitro EC activation assays

Medium was conditioned by $TIE2^-$ monocytes or TEMs for 24 hours and then incubated with 20 μmol/L MMP-9 Inhibitor I (Calbiochem), which inhibits MMP-1, MMP-9, and MMP-13, or 0.4% DMSO (vehicle control) for 1 hour at 37°C. The water-soluble thymidine phosphorylase (TP) inhibitor AEAC (6-[2-aminoethyl]amino-5-chlorouracil; 25 μmol/L; a gift from Dr. Edward Schwartz, Albert Einstein College of Medicine, Bronx, NY; refs. 28, 29) was incubated with sorted monocyte populations 1 hour before exposure to 300 ng/mL ANG-2, and then medium was collected after 24 hours. For the tubule formation assay, serum-starved human umbilical vein ECs (HUVEC; 8,000 cells/96-well) were resuspended in conditioned medium and seeded onto growth factor–reduced Matrigel (BD Biosciences). After 6 hours, tubule formation was measured using ImageJ software. For the spheroid/spouting assay, HUVEC spheroids (400 cells) were generated as described previously (30) and incubated for 24 hours with conditioned media. Images of sprouting spheroids were taken with an Axiovert 100M microscope and Plan-NEOFLUAR 10×/0.30 objective lens. Capillary sprouting length was quantified using AxioVision Rel 4.4 digital imaging software (Zeiss). Every sprout from 10 spheroids per group was measured, and the mean cumulative sprout length was calculated. Both sets of *in vitro* assays were performed three times.

Immunoprecipitation and immunoblot analysis

Serum-starved HUVECs (2×10^6) or human monocytes (2×10^7) were treated with 300 ng/mL ANG-2. Cells were lysed in 50 mmol/L Tris and 100 mmol/L NaCl with 1% Triton X-100 containing protease and phosphatase inhibitors. After spinning at 14,000 rpm for 10 minutes, supernatant was collected. Protein lysates (40 μg) were precleared with protein A/G beads (Santa Cruz Biotechnology) and then incubated with 5 μg anti-TIE2 (clone 83711; R&D Systems) overnight at 4°C. Protein A/G beads were added for 2 hours at 4°C. IgG–protein A/G complexes were collected by centrifugation,

washed, and boiled in loading buffer before loading into 8% SDS-polyacrylamide gels. Separated proteins were transferred to nitrocellulose, blocked with 5% milk in TBS–Tween 20, and probed with anti–phospho-TIE2 (0.5 μg/mL; Y992; R&D Systems) overnight at 4°C. Membranes were washed and incubated with biotin-conjugated anti-rabbit antibodies (1:5,000; R&D Systems) for 1 hour at room temperature, followed by streptavidin–horseradish peroxidase (HRP; 1:200; R&D Systems) for 1 hour at room temperature. Bands were visualized by enhanced chemiluminescence (Amersham). Membranes were then stripped and reprobed with anti-TIE2 (1:250; clone 83711; R&D Systems) followed by HRP-conjugated goat anti-mouse antibodies (1:5,000; Dako). Similar experiments were repeated three times using three different blood donors.

For detection of TP, adherent human monocytes were treated with 300 ng/mL ANG-2, washed in cold PBS, and lysed. Proteins were separated on 10% SDS-polyacrylamide gels and transferred onto nitrocellulose. The remainder of the procedure was carried out as above using anti-TP antibodies (1:1,000; clone P-GF.44C) purchased from Abcam followed by anti-mouse secondary.

Murine tumor model

TIE1-tTA–driven h*Ang-2* double-transgenic (DT) mice were generated as previously described (Supplementary Fig. S4A; refs. 31, 32). Mice were depleted of doxycycline 2 weeks before implantation of tumor cells (Supplementary Fig. S4B). Syngeneic Lewis lung carcinoma (LLC) cells (2×10^6) were inoculated s.c. and allowed to propagate for 2 weeks. Caliper measurements were taken every 3 days, and tumor volume was calculated with the following formula: length × width^2/2. Each group consisted of at least five mice and experiments were repeated four times. Animals were cared for in accordance with German Legislation on the Care and Use of Laboratory Animals.

Immunohistochemistry and immunofluorescence confocal microscopy

Detection of blood vessels and pericytes, assessment of MVD, and pericyte coverage were performed as described previously (33) using rat anti-mouse CD31 (BD Biosciences) and anti–α-smooth muscle actin (αSMA; Sigma). CD45, Gr-1, CD3, and B220 antibodies were purchased from BD Biosciences. Images were taken with a Nikon 80i microscope, and staining was analyzed with Soft Imaging Analysis System software at ×10 magnification. ApopTag In Situ Apoptosis Detection kit (Chemicon) was used as before (33). Assessment of hypoxic tumor regions was conducted as described previously (27) using Hypoxyprobe (HPI).

Detection of F4/80$^+$TIE2$^-$ TAMs and TEMs was performed using FITC-conjugated anti-F4/80 (1:25, clone CI: A3-1; AbD Serotec) and phycoerythrin-conjugated anti-murine TIE2 (1:50; eBioscience). Anti–MMP-9 (1:500; a gift from Dr. Zena Werb, University of California, San Francisco, San Francisco, CA), anti–cathepsin B (CTSB; 15 μg/mL; R&D Systems), anti-TP (1:500; Abcam), and anti-MRC1 (1:25; R&D Systems) antibodies were detected by Alexa Fluor 647–conjugated anti-goat or anti-rabbit secondary antibodies (1:500; Invitrogen). The anti–hANG-2 antibody (clone 180102) was from R&D Systems and used at 1:500. TP and ANG-2 antibodies were preabsorbed with secondary antibodies before incubation with tissue. Tumor vasculature was identified using APC-conjugated anti-CD31 (1:50; eBioscience). Nuclei were highlighted using 30 nmol/L 4′,6-diamidino-2-phenylindole (DAPI; Invitrogen) for 2 minutes. Images were captured using a Zeiss LSM 510 laser scanning confocal microscope. Further details about microscopy can be found in the Supplementary Data.

Statistical analysis

Student's two-tailed *t* test (paired or unpaired as appropriate) or one-way ANOVA was used to determine *P* values using GraphPad Prism software. A *P* value of <0.05 was considered statistically significant. All data shown are mean ± SE.

Results

Human TEMs are more proangiogenic than TIE2$^-$ monocytes *in vitro*

Human TEMs and TIE2$^-$ monocytes were isolated from peripheral blood by FACS (Supplementary Fig. S1A), and increased *TIE2* expression in TEMs was confirmed using quantitative real-time PCR (qPCR; Supplementary Fig. S1B). Interestingly, flow cytometry revealed that, unlike ECs, TIE1 expression on both monocyte subpopulations was negligible (Supplementary Fig. S2).

In the EC spheroid/sprouting assay, we found that TEMs induced significantly more sprouts than TIE2$^-$ monocytes (Fig. 1A). In the tubule formation assay, TEM-conditioned medium also significantly increased EC tubule length (Fig. 1B) and tubule area (47.9 ± 3.7 versus 32.5 ± 2.8 μm^2; $P = 0.02$; data not shown) when compared with TIE2$^-$ monocyte-conditioned medium. Furthermore, addition of an MMP inhibitor significantly reduced the formation of tubules by TEMs (33.8 ± 3.6% reduction for length, 23.4 ± 4.1% reduction for area) but not TIE2$^-$ monocytes (data not shown).

We then used qPCR to examine mRNA expression levels of various tumor-promoting and M2 (i.e., alternatively activated macrophage)–associated genes, including proangiogenic factors (*MMP-9, VEGF, EGF, FGF2, COX-2, CTSB, WNT5A*, and *TP/ECGF1*), immunomodulatory cytokines (*TNFα, IL-1β, IL-6, IL-8*, and *IL-10*), cell adhesion molecule (*ICAM-1*), and cell surface receptors [mannose receptor (*MRC1*), *CXCR4, TLR-2*, and *TLR-4*]. TEMs expressed significantly higher levels of MMP-9 (Fig. 1C). Densitometric analysis of gelatin zymography showed a significant difference between the amount of pro–MMP-9 released by the cells (Fig. 1C), with TEMs producing more pro–MMP-9 than TIE2$^-$ monocytes (421.3 ± 42.1 versus 570.8 ± 57.1 relative units; $P = 0.047$; data not shown). MMP-2 activity was not detected.

In addition to *MMP-9*, TEMs expressed higher levels of *VEGFA* mRNA and released higher levels of VEGFA and TNFα protein than TIE2$^-$ monocytes (Fig. 1C). TEMs expressed higher levels of *COX-2, MRC1*, and *WNT5A*

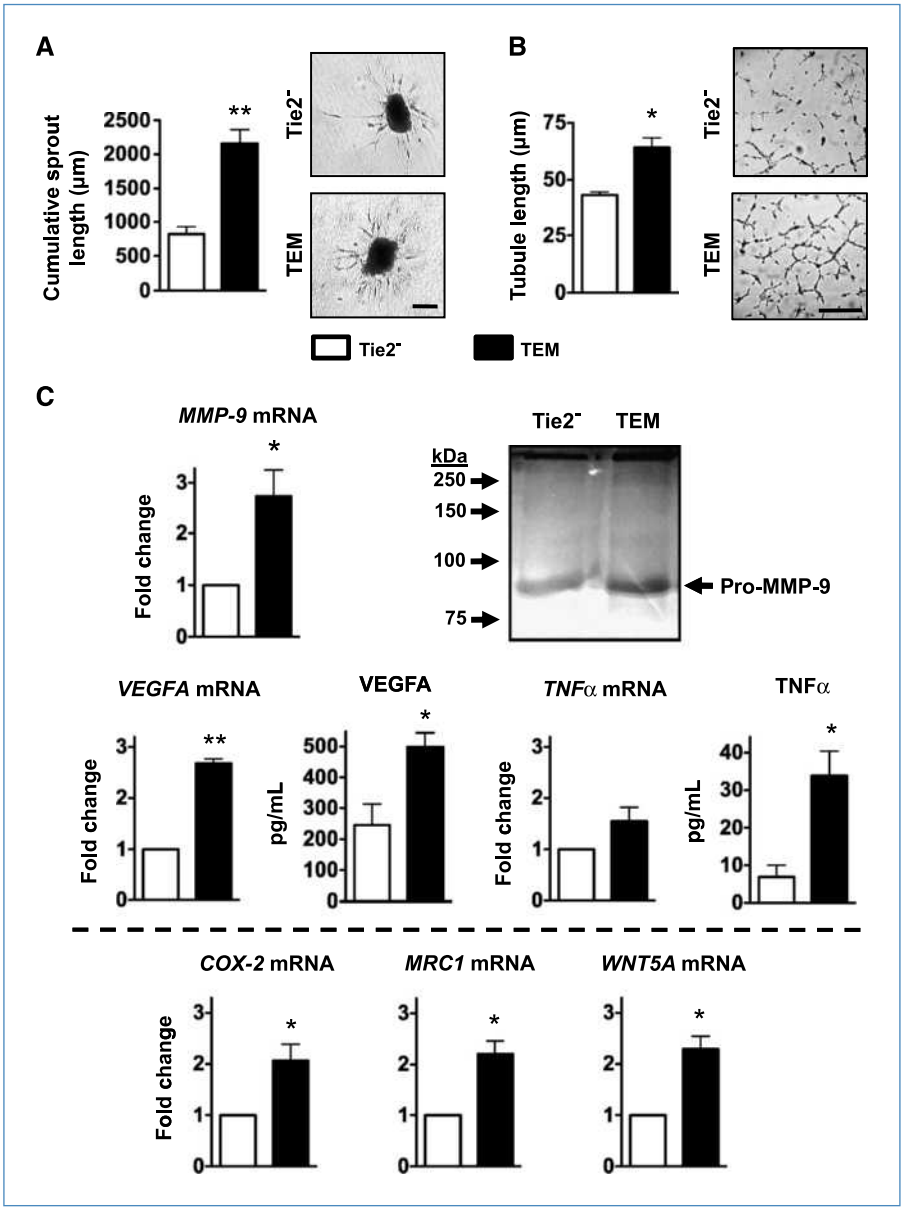

Figure 1. Circulating human TEMs are inherently more angiogenic than TIE2⁻ monocytes. Conditioned medium was collected from sorted $CD14^+TIE2^-$ and $CD14^+TIE2^+$ (TEMs) human monocyte subpopulations and used in either a HUVEC sprouting assay (A) or a HUVEC tubule formation assay *in vitro* (B). TEMs induced significantly more EC activation than TIE2⁻ monocytes in both assays. C, RNA was isolated from monocyte subpopulations and analyzed by qPCR. Cells were also cultured and conditioned medium was assayed for pro–MMP-9 by gelatin zymography or VEGF and TNFα by cytometric bead array. Top, *VEGF* and *TNFα* mRNA levels assayed by qPCR, and their corresponding proteins; bottom, *COX-2, MRC1*, and *WNT5A* mRNA levels. *, $P < 0.05$; **, $P < 0.01$, compared with TIE2⁻ monocytes. Data from at least three replicate assays shown. Scale bars, 50 μm.

mRNA (Fig. 1C) but significantly lower levels of *EGF* mRNA (−1.7 ± 0.1 fold difference; $P = 0.007$; data not shown) and protein (13.2 ± 3.2 versus 4.6 ± 1.2 pg/mL; $P = 0.035$; data not shown) than TIE2⁻ monocytes. Expression of *CTSB, CXCR4, TP, ICAM-1, IL-1β, IL-6, IL-8, IL-10, TLR2, TLR4*, or *TNFα* mRNA was not significantly different between the two populations. *FGF2* mRNA was not detected in either subset.

Agonistic effects of ANG-2 on human TEMs *in vitro*

To investigate the possible effect of ANG-2 on the phenotype and function of TEMs, we first exposed freshly isolated human monocytes and HUVECs to ANG-2 and examined phosphorylation of TIE2. Activation typically occurred within 10 minutes of ANG-2 stimulation in both cell types, as variation between monocyte donors was minimal (Fig. 2A). Densitometry revealed a 50% increase in phosphorylation at 10 minutes for monocytes.

Although expression of *VEGF* and *MMP-9* mRNA was not further increased by ANG-2 in TEMs (Fig. 2B), it significantly upregulated expression of two other proangiogenic enzymes, *CTSB* and *TP* (Fig. 2B and C), an effect not seen in TIE2⁻ cells. Increased TP protein levels were confirmed by Western blot following exposure to ANG-2 (Fig. 2C).

The ability of ANG-2 to further enhance the inherent proangiogenic functions of TEMs was then assessed. ANG-2 treatment of TIE2⁻ monocytes failed to augment their relatively low capacity to induce EC sprouts or tubule formation (data not shown), whereas ANG-2 significantly increased the ability of TEMs to activate ECs in both assays (Fig. 2D). This

stimulatory effect (64% increase for cumulative sprout length, 39% increase for tubule length, and 91% increase for tubule area) is greater than that reported previously for VEGF and FGF2 (34). Exposure of TEMs to a specific TP inhibitor had no effect on cell viability (data not shown) but significantly reduced their ability to activate ECs in response to ANG-2 (Fig. 2D).

In addition to *CTSB* and *TP*, ANG-2 also significantly upregulated the expression of the two M2-associated genes, *IL-10* and *MRC1*, by TEMs (Fig. 3A and B, left). IL-10 protein levels were significantly higher in TEM-conditioned medium following ANG-2 treatment (Fig. 3A, right), and flow cytometry showed an increase in MRC1 expression on TEMs following ANG-2 treatment (Fig. 3B, right). Both the percentage of TEMs expressing MRC1 [control (11.0 ± 5.3%) versus ANG-2 (17.1 ± 5.4%)] and the median fluorescence intensity [MFI; control (1,399 ± 58.1 arbitrary units) versus ANG-2 (1,918 ± 220.6 arbitrary units)] were significantly higher in the ANG-2–treated group ($P = 0.0012$ and 0.045, respectively). TEM expression of *IL-6* mRNA was significantly reduced following ANG-2 stimulation; however, the amount of IL-6 secreted was not significantly different following ANG-2 treatment of TEMs (Fig. 3C). *CCL17* mRNA was also significantly increased in TEMs by ANG-2 (2.7 ± 0.9 fold increase; $P = 0.013$; data not shown). All the other mRNA species screened by qPCR (*EGF, COX-2, WNT5A, TNFα, IL-1β, IL-6, IL-8, ICAM-1, CXCR4, TLR-2*, and *TLR-4*) were not altered by ANG-2 in either population (data not shown). Of note, only TEMs, not TIE2$^-$ monocytes, responded to ANG-2, indicating that the TIE2 receptor is required for its effects on TEMs.

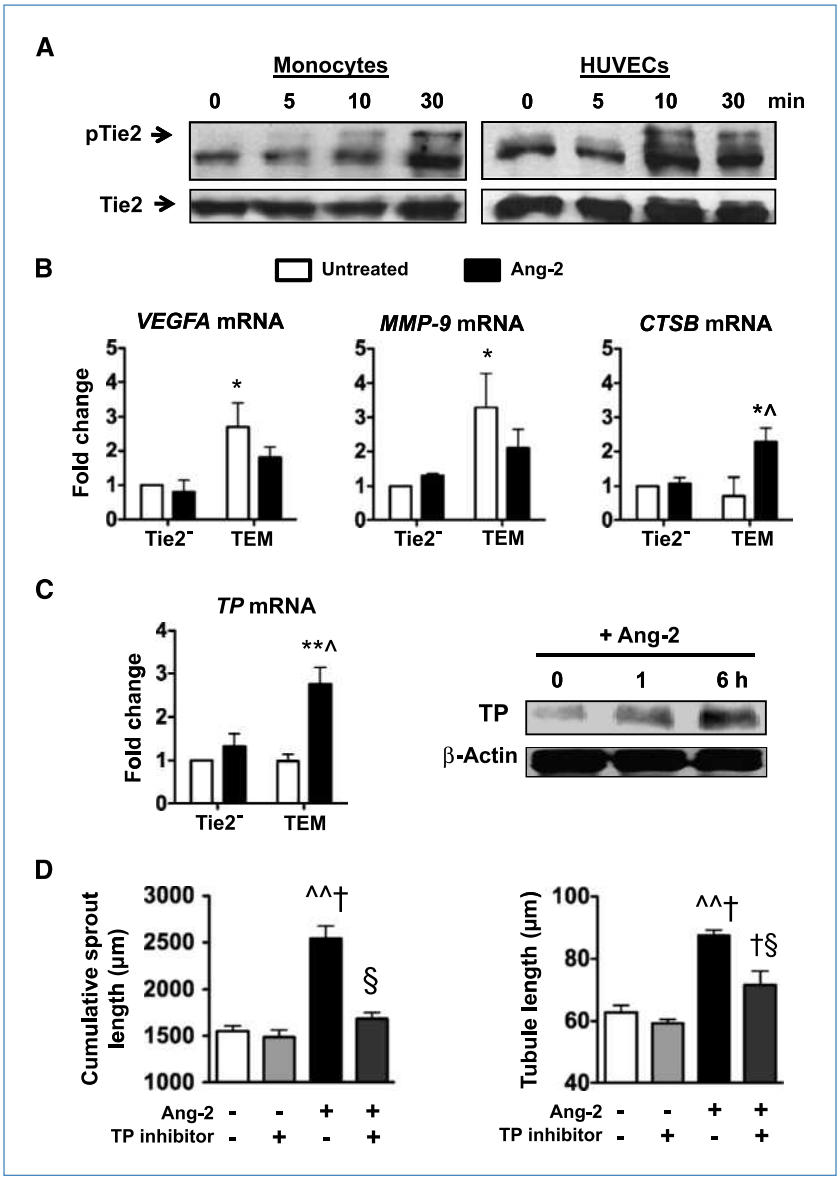

Figure 2. ANG-2 induces phosphorylation of TIE2 and enhances the proangiogenic ability of human TEMs *in vitro*. A, human monocytes and HUVECs were exposed to 300 ng/mL of recombinant ANG-2, TIE2 was then immunoprecipitated from cell lysates, and phosphorylation was analyzed by immunoblotting. B, qPCR analysis of *VEGF, MMP-9*, and *CTSB* mRNA. C, upregulation of *TP* expression by ANG-2 as assessed by qPCR and immunoblotting. D, HUVEC sprouting assay (left) and tubule formation (right) after incubation with conditioned medium from untreated or ANG-2–treated TEMs. Where indicated, cells were preincubated with 25 μmol/L TP inhibitor (AEAC) before exposure to ANG-2. *, $P < 0.05$; **, $P < 0.01$, compared with TIE2$^-$ monocytes. ^, $P < 0.05$; ^^, $P < 0.01$, compared with untreated TEMs; †, $P < 0.05$, compared with untreated TEMs + TP inhibitor; §, $P < 0.05$, compared with ANG-2–treated TEMs. Data from at least four replicate assays shown. Sprouting assay data are representative of three independent experiments.

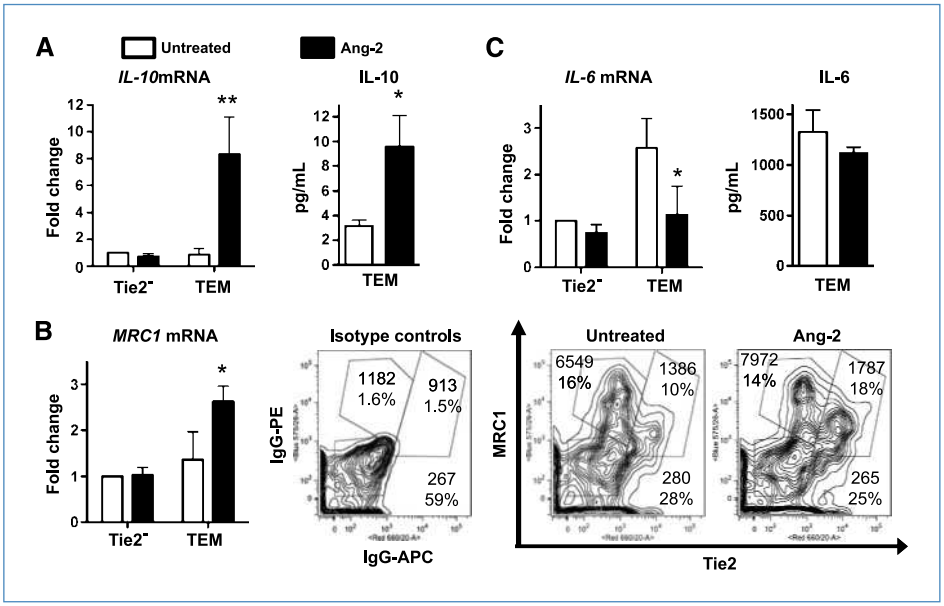

Figure 3. ANG-2 upregulates expression of two classic M2 genes by human TEMs: IL-10 and MRC1. A to C, left, mRNA levels as determined by qPCR; right, cytometric bead array analysis of soluble protein in TEM-conditioned medium. B, right, flow cytometry analysis of MRC1 cell surface expression. Figures cited on the contour maps indicate MFI of MRC1 expression and the proportion of MRC1$^+$ cells in each gate. Pooled data from at least three replicate experiments shown. *, $P < 0.05$; **, $P < 0.01$, compared with untreated TEMs.

Differential effects of ANG-1 on human TEMs *in vitro*

Unlike ANG-2, ANG-1 had no effect on *TP, MRC1, IL-10*, or *CTSB* mRNA levels in TEMs but significantly downregulated *CCL17* mRNA and upregulated *EGF* mRNA levels (Supplementary Fig. S3). Like ANG-2, only TEMs responded to ANG-1, indicating that the TIE2 receptor is required for its effects on TEMs.

Effects of ANG-2 overexpression on the growth and vasculature of LLC tumors *in vivo*

We used a DT mouse model in which the vasculature specifically overexpresses hANG-2—termed ANG-2 DT (Supplementary Fig. S4A; ref. 32). LLCs were grown s.c. in these mice, and upregulation of hANG-2 in plasma was confirmed using ELISA (Supplementary Fig. S4C). The EC-specific upregulation of hANG-2 was validated by the immunofluorescent labeling of CD31, TIE2, and hANG-2 in LLCs (Supplementary Fig. S4D). Approximately 60% to 70% of CD31$^+$ blood vessels expressed hANG-2 in ANG-2 DT tumors, with negligible expression seen in LLC grown in wild-type (WT) mice.

Although tumor volumes were not significantly different between WT and ANG-2 DT mice (Supplementary Fig. S5A), excised tumors from the latter group were more hemorrhagic than those grown in WT mice (Supplementary Fig. S5B) and contained significantly higher numbers of CD31$^+$ microvessels (Fig. 4A). The vessels in ANG-2 DT tumors exhibited an immature phenotype (i.e., little or no pericyte coverage) and displayed increased levels of EC apoptosis (Fig. 4A). This accords well with the finding that ANG-2 DT tumors were more hypoxic than WT tumors (Fig. 4A).

Overexpression of ANG-2 increases TEM infiltration into tumors

As we previously showed that ANG-2 is a potent chemoattractant for human TEMs *in vitro* (3, 4), we investigated whether TEM infiltration into tumors was altered by hANG-2 overexpression. Immunohistochemistry showed that CD45$^+$ leukocyte tumor infiltration (assessed as a proportion of total tumor area) was significantly increased in ANG-2 DT compared with WT tumors, with the majority of these cells being F4/80$^+$ macrophages (Supplementary Fig. S5C). Similarly, immunofluorescent analysis replicated this increase in F4/80$^+$ macrophages but also found a greater increase in the proportion of F4/80$^+$TIE2$^+$ cells (TEMs) than F4/80$^+$TIE2$^-$ TAMs in ANG-2 DT tumors, suggesting selective recruitment of TEMs (Fig. 4B). These data were confirmed by flow cytometry analysis of enzymatically dispersed tumors (data not shown). The frequency of other leukocytes was unaffected, including Gr-1$^+$ cells, CD3$^+$ T cells, and B220$^+$ B cells (data not shown). No differences in any leukocyte subsets were seen between normal tissues (i.e., brain, heart, and spleen) of WT and ANG-2 DT mice (data not shown).

TEM phenotype is affected by ANG-2 overexpression *in vivo*

A significantly greater number of MMP-9–expressing TEMs but not TIE2$^-$ TAMs were present in Ang-2 DT than WT tumors (Fig. 5A). This could be explained by the fact that virtually all TEMs—and <10% F4/80$^+$TIE2$^-$ TAMs—expressed MMP-9 in both tumor types, and this difference in MMP-9 expression between these two macrophage populations was significant (Fig. 5A). In agreement with our *in vitro* studies, ANG-2 overexpression had no effect on the level of MMP-9 expression/TEM as assessed by the MFI per cell (Fig. 5A).

The frequency of MRC1$^+$ TEMs was also greater in ANG-2 DT tumors than WT, with MRC1 expression being largely confined to TEMs and absent in F4/80$^+$TIE2$^-$ TAMs (Fig. 5B). Figure 6 shows that the majority of both TEMs and TIE2$^-$ TAMs expressed CTSB and TP, but both were more abundant in ANG-2 DT tumors (due to increased numbers of TEMs and TIE2$^-$ TAMs in ANG-2 DT tumors).

Moreover, the expression of MRC1 (Fig. 5B), CTSB (Fig. 6A), and TP (Fig. 6B) per TEM was significantly increased in ANG-2 DT tumors.

Discussion

Myeloid cells are essential for blood vessel formation, maintenance, and function in tumors (35), and TEMs are one of the most proangiogenic subsets of these cells (1, 4, 5). It has previously been suggested that circulating human or mouse TEMs may be innately proangiogenic, as mice inoculated with tumor cells and TEMs form more vascularized tumors than those injected with tumor cells alone (1, 4). In the present study, we confirm that circulating human TEMs are indeed more proangiogenic than TIE2$^-$ monocytes and express higher levels of such potent proangiogenic factors as *MMP-9, VEGF, COX-2*, and *WNT5A*. Interestingly, we also found that MMP-9 was widely expressed by the vast majority (>90%) of TEMs in tumors. Use of an MMP-9 inhibitor *in vitro* suggests that this enzyme plays an important role in mediating the innate, proangiogenic function of circulating TEMs. However, it should be noted that this inhibitor also reduces MMP-1 and MMP-13 activities, so the relative contribution of these three enzymes awaits further study.

We reported previously that ANG-2 is a chemoattractant for human TEMs *in vitro*, an effect mediated by TIE2 (3, 4). Our data here show that ANG-2 overexpression by the tumor vasculature results in greater infiltration of murine TEMs into tumors. This observation could be due to the direct chemotactic effect of ANG-2 on TEMs and/or the increased number of blood vessels present in ANG-2 DT tumors, allowing TEMs and other leukocytes greater access into tumors. At first glance, the latter possibility seems to be supported

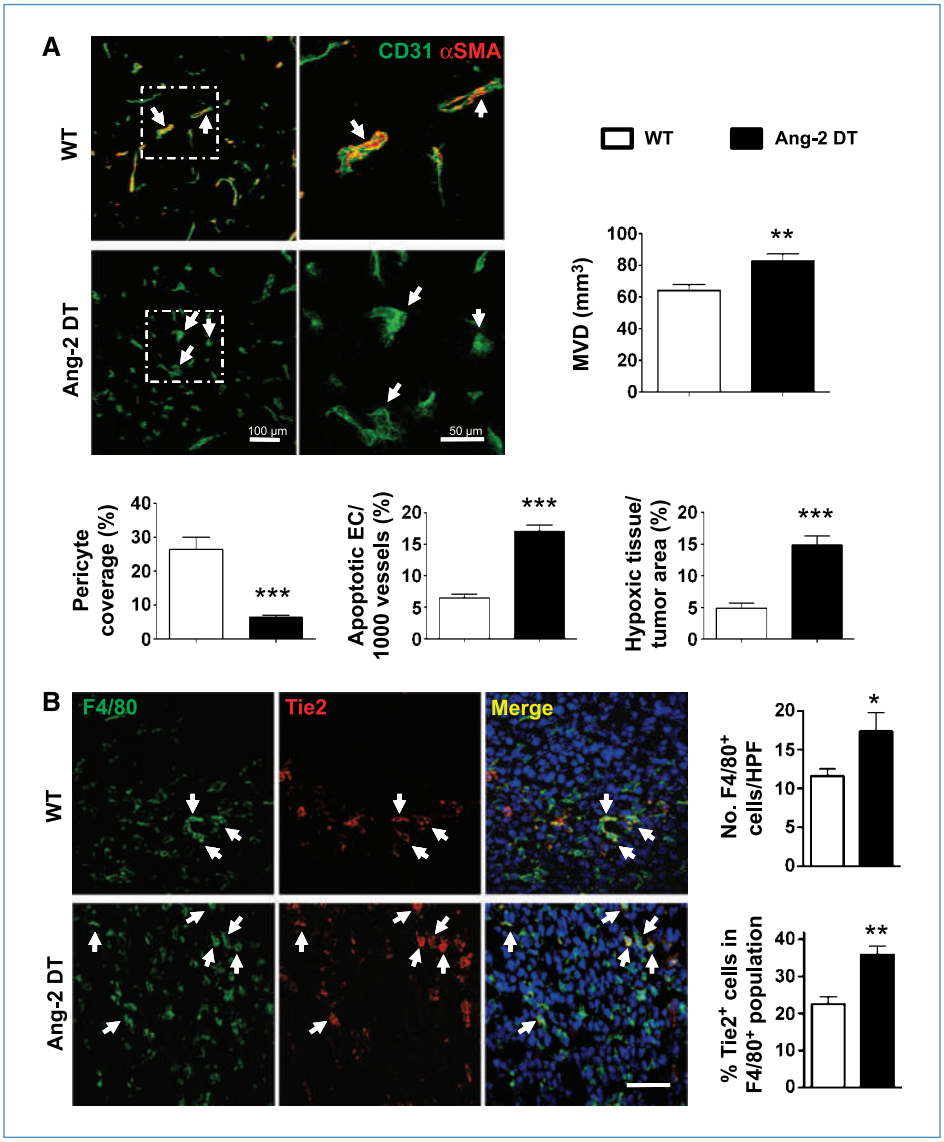

Figure 4. Tumors grown in ANG-2–overexpressing mice contain more immature microvessels and increased numbers of F4/80$^+$ macrophages and TEMs. hANG-2 expression in ECs was achieved using a DT Tet-Off expression system. LLC cells were allowed to propagate for 2 wk. A, the vascular phenotype of ANG-2 DT and WT LLC tumors was assessed by CD31/αSMA double immunofluorescence. αSMA$^+$ pericytes are denoted by white arrows. For pericyte quantification, 10^3 CD31$^+$ vessels per tumor were analyzed and percentage of αSMA$^+$ pericyte coverage was determined. MVD was determined by CD31 immunohistochemistry and quantified by Soft Imaging Analysis System software. EC apoptosis was determined by the terminal deoxynucleotidyl transferase–mediated dUTP nick end labeling assay coupled with CD31 immunohistochemistry. Regions of hypoxia were identified using anti-PIMO antibody, analyzed by NIS Elements software, and represented as a percentage of the entire tumor area. B, LLC tumor sections were immunofluorescently double labeled with F4/80- and TIE2-specific antibodies. Scale bar, 50 μm. Arrows denote TEMs in representative images. The total F4/80$^+$ (including both TIE2$^-$ and TIE2$^+$) macrophage population and TEM subpopulation were quantified from six high-powered fields (HPF) for each tumor section. Data are pooled from five tumors per group at minimum. *, $P < 0.05$; **, $P < 0.01$; ***, $P < 0.005$, compared with WT tumors.

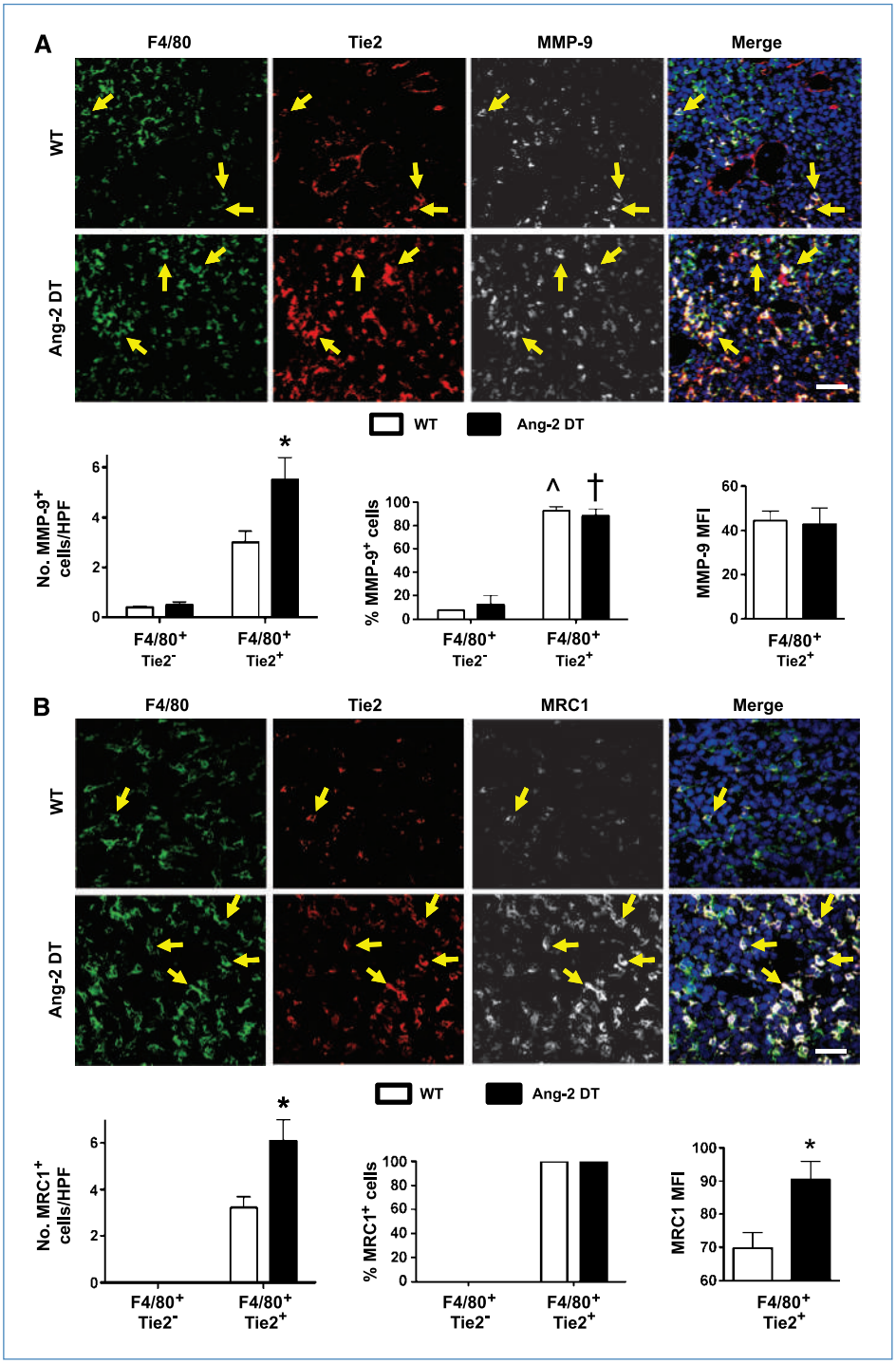

Figure 5. TEMs are the main source of MMP-9 and MRC1 in both WT and ANG-2–overexpressing tumors. Frozen sections of LLC tumors grown in WT or ANG-2 DT mice were stained with F4/80 (green), TIE2 (red), and either (A) MMP-9 or (B) MRC1 antibodies (both white) and then analyzed by fluorescence confocal microscopy. Representative images are shown for each antigen alone as well as merged images (DAPI, blue). MMP-9 or MRC1–expressing TEMs are denoted by arrows. The number of MMP-9–expressing or MRC1-expressing TEMs per HPF, the percentage of $F4/80^+TIE2^-$ and $F4/80^+TIE2^+$ TAM populations expressing MMP-9 or MRC1, as well as the MFI of MMP-9/MRC1 expression by TEMs are represented graphically. $TIE2^+F4/80^-$ structures are blood vessels. *, $P < 0.05$, compared with $F4/80^+TIE2^+$ cells in WT tumors; ^, $P < 0.05$; †, $P < 0.05$, compared with $F4/80^+TIE2^-$ cells in WT and ANG-2 DT tumors, respectively. Scale bar, 50 μm.

by our finding that the frequency of all $CD45^+$ leukocytes was increased in ANG-2 DT tumors. However, the majority of $CD45^+$ cells were $F4/80^+$ TAMs and TEMs, whereas the number of $Gr\text{-}1^+$ granulocytes, T cells, and B cells was not increased in ANG-2 DT tumors. The enhanced recruitment of TEMs may also be due to the increased level of tumor hypoxia seen in ANG-2 DT tumors, as hypoxia-induced CXCL12 attracts increased numbers of TEMs into tumors (36).

Here, we confirm that ANG-2 stimulates TIE2 receptor phosphorylation in human TEMs and upregulates their expression of several tumor-promoting factors. This result may seem unexpected given that some *in vitro* studies report

that ANG-2 simply inhibits or dampens TIE2 signaling in response to ANG-1 in ECs (7). However, as mentioned previously, tumors often produce higher levels of ANG-2 than ANG-1 (10, 14–20), so the antagonistic role of ANG-2 on ANG-1 signaling is likely minimal in such tissues. Moreover, agonistic effects of ANG-2 on ECs and its ability to phosphorylate TIE2—even in the absence of ANG-1—have been reported (37, 38). TIE1 receptors on ECs can also modulate the effect of angiopoietins on TIE2 (39–41), although the agonistic effects of ANG-2 do not involve TIE1 (39, 41). As TIE1 is absent on TEMs, the agonistic effects of ANG-2 reported here also seem to be independent of TIE1.

We show that exposure to ANG-2 enhances the angiogenic potential of human TEMs *in vitro* by augmenting expression of two proangiogenic genes: *TP* and *CTSB*. TP catalyzes the breakdown of thymidine that forms a proangiogenic sugar,

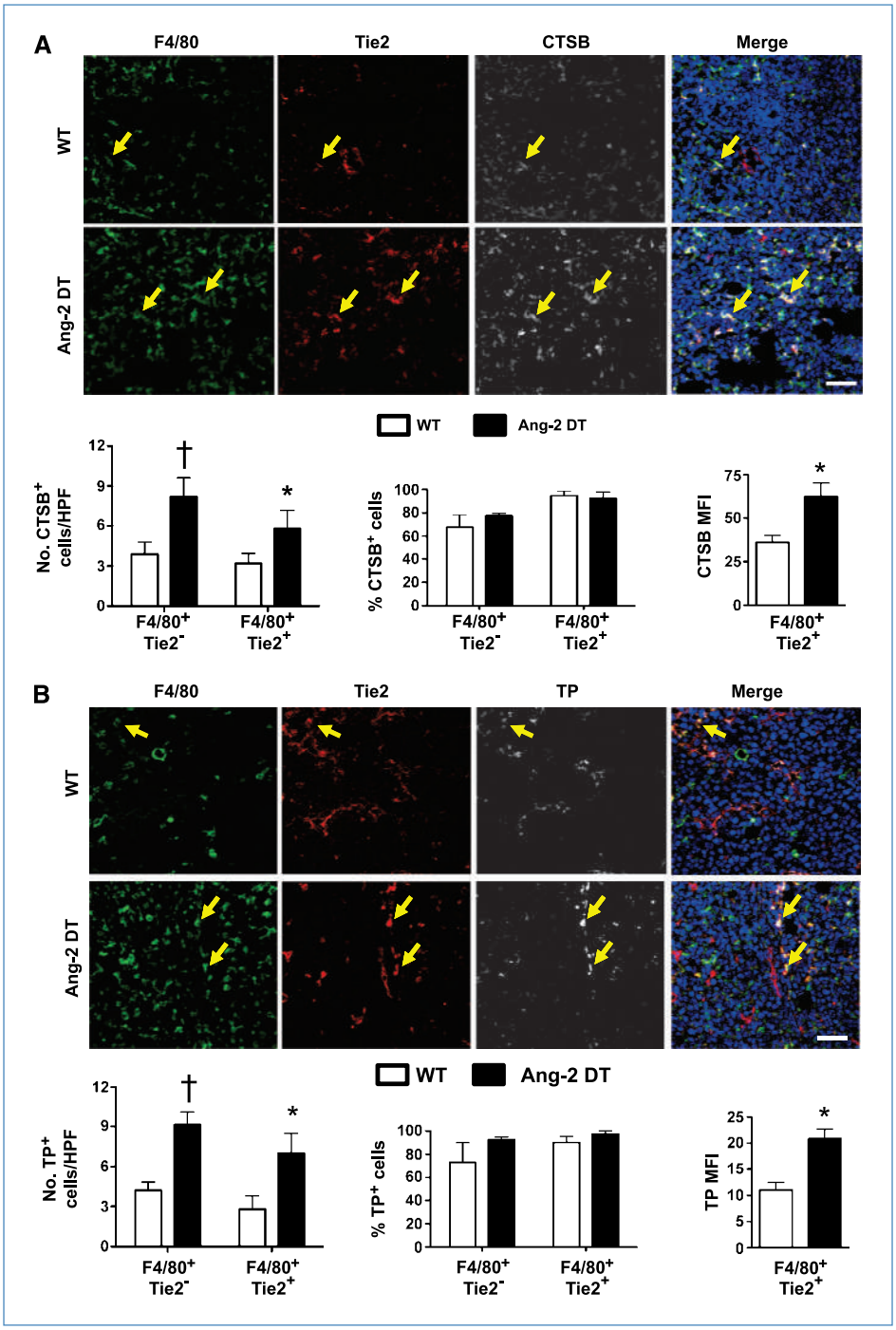

Figure 6. TEMs upregulate both CTSB and TP in ANG-2–overexpressing tumors. LLC tumor sections from WT or ANG-2 DT mice were stained with F4/80 (green), TIE2 (red), and CTSB (white, A) or TP (white, B) antibodies and then analyzed by fluorescence confocal microscopy. Representative images are shown for each antigen alone as well as merged images (DAPI, blue). CTSB- or TP-expressing TEMs are denoted by arrows. The number of $CTSB^+$ and TP^+ macrophage subpopulations per HPF is represented graphically. The percentage of $F4/80^+TIE2^-$ and $F4/80^+TIE2^+$ TAM populations expressing each protein and the MFI per TEM are also shown. $TIE2^+F4/80^-$ structures are blood vessels. *, $P < 0.05$, compared with $F4/80^+TIE2^+$ cells in WT tumors; †, $P < 0.05$, compared with $F4/80^+TIE2^-$ cells in WT tumors. Scale bar, 50 μm.

2-deoxy-D-ribose (42). Previously, we and others reported that human TAMs express TP and that this correlates positively with tumor angiogenesis (43, 44). CTSB expression in human cancers has also been implicated in tumor progression and poor prognosis (reviewed in ref. 45). Recently, TAMs have been shown to be the major source of CTSB in various tumor models, and the proteolytic activity of this enzyme is critical for tumor growth, angiogenesis, and invasion (46, 47). Consistent with our *in vitro* results using human TEMs, murine TEMs in ANG-2 DT tumors exhibited greater expression of TP and CTSB than in WT tumors. ANG-2 upregulation of both TEM infiltration into tumors and their expression of such proangiogenic enzymes could explain the increased number of microvessels in ANG-2 DT compared with WT tumors. However, the tumor-promoting effect of these activated TEMs may have been countered by the direct deleterious effect of ANG-2 overexpression on the maturity and viability of ECs in ANG-2 DT mice, resulting in similar growth between tumor types.

We previously showed that human TEMs respond to ANG-2 by decreasing their expression of TNFα and IL-12 (3). We report here that ANG-2 further stimulates their high basal level of MRC1 *in vitro*. Although care needs to be taken when comparing the responses to ANG-2 of human blood TEMs *in vitro* with those of murine tumor TEMs *in vivo*, it is interesting to note that MRC1 expression by murine TEMs was higher in ANG-2 DT than WT tumors. We also found that ANG-2 upregulated the expression of the potent immunosuppressive factor IL-10 and the regulatory T-cell (Treg) chemokine CCL17. Interestingly, high levels of IL-10, CCL17, and MRC1 coupled with low levels of TNFα, IL-12, and IL-6 expression are indicative of an alternative ("M2") activation status in macrophages, a phenotype commonly associated with TAMs (48, 49). Furthermore, Pucci and colleagues (5) recently reported that murine tumor TEMs express a pronounced M2 phenotype. Our data indicate that ANG-2 in tumors may drive this M2-like polarization of TEMs. By contrast, ANG-1 induced a completely different gene expression profile from that seen with ANG-2, suggesting that TEMs can be skewed away from an M2-like phenotype in tissues where ANG-1 is more abundant.

In our study, high levels of ANG-2 expressed by the tumor vasculature seem to act in an autocrine manner, causing vascular disruption, as shown by increased EC apoptosis and consequent tumor hypoxia. Such antivascular effects of high-dose ANG-2 may override the enhanced, proangiogenic activity of ANG-2–stimulated TEMs. However, such effects of ANG-2 may be dose dependent and it is possible that lower levels of ANG-2 in tumors might have less pronounced antivascular effects so that ANG-2–stimulated TEMs would then induce further tumor angiogenesis and progression. On the other hand, the genetic knockout of *Ang-2* in tumor models increases vascular maturation and pericyte coverage, resulting in an "angiostatic" phenotype, possibly from the enhanced availability of TIE2 to bind ANG-1 in the absence of ANG-2 (26). Our data (Supplementary Fig. S3) also suggest that, in the absence of ANG-2, ANG-1 stimulation of TEMs would not induce a proangiogenic or tumor-promoting phenotype. It will be interesting to investigate the effects of depleting ANG-2 in tumors on these two cell types using new-generation anti–ANG-2 inhibitors (50). Such studies are now warranted to see whether the ANG-2/TEM axis is a suitable target for anticancer therapy, as drugs that selectively target the ANG-2–TIE2 interaction may impair the biological activity of both angiogenic ECs and proangiogenic TEMs in the tumor microenvironment. However, it also remains to be seen whether other tumor-derived signals also contribute to shaping the proangiogenic activity and the insidious functions of TEMs in tumors.

Disclosure of Potential Conflicts of Interest

No potential conflicts of interest were disclosed.

Acknowledgments

We thank Dr. Dan Dumont for the ANG-2 DT mice, Dr. Zena Werb for the MMP-9 antibody, Dr. Edward Schwartz for the TP inhibitor, and Susan Newton and Kay Hopkinson (University of Sheffield Flow Cytometry Core Facility).

Grant Support

Breast Cancer Campaign, UK (C.E. Lewis, C. Murdoch, and M. De Palma) and German Research Foundation grant SFB/TR23 [Y. Reiss, K.H. Plate (Project C1), and C. Urbich (Project B5)].

The costs of publication of this article were defrayed in part by the payment of page charges. This article must therefore be hereby marked *advertisement* in accordance with 18 U.S.C. Section 1734 solely to indicate this fact.

Received 01/05/2010; revised 04/09/2010; accepted 04/30/2010; published OnlineFirst 06/08/2010.

References

1. De Palma M, Venneri MA, Galli R, et al. Tie2 identifies a hematopoietic lineage of proangiogenic monocytes required for tumor vessel formation and a mesenchymal population of pericyte progenitors. Cancer Cell 2005;8:211–26.
2. De Palma M, Venneri MA, Roca C, Naldini L. Targeting exogenous genes to tumor angiogenesis by transplantation of genetically modified hematopoietic stem cells. Nat Med 2003;9:789–95.
3. Murdoch C, Tazzyman S, Webster S, Lewis CE. Expression of Tie-2 by human monocytes and their responses to angiopoietin-2. J Immunol 2007;178:7405–11.
4. Venneri MA, De Palma M, Ponzoni M, et al. Identification of proangiogenic TIE2-expressing monocytes (TEMs) in human peripheral blood and cancer. Blood 2007;109:5276–85.
5. Pucci F, Venneri MA, Biziato D, et al. A distinguishing gene signature shared by tumor-infiltrating Tie2-expressing monocytes, blood "resident" monocytes, and embryonic macrophages suggests common functions and developmental relationships. Blood 2009;114:901–14.
6. Davis S, Aldrich TH, Jones PF, et al. Isolation of angiopoietin-1, a ligand for the TIE2 receptor, by secretion-trap expression cloning. Cell 1996;87:1161–9.
7. Maisonpierre PC, Suri C, Jones PF, et al. Angiopoietin-2, a natural

antagonist for Tie2 that disrupts *in vivo* angiogenesis. Science 1997; 277:55–60.
8. Kim I, Moon SO, Koh KN, et al. Molecular cloning, expression, and characterization of angiopoietin-related protein. angiopoietin-related protein induces endothelial cell sprouting. J Biol Chem 1999;274: 26523–8.
9. Valenzuela DM, Griffiths JA, Rojas J, et al. Angiopoietins 3 and 4: diverging gene counterparts in mice and humans. Proc Natl Acad Sci U S A 1999;96:1904–9.
10. Augustin HG, Koh GY, Thurston G, Alitalo K. Control of vascular morphogenesis and homeostasis through the angiopoietin-Tie system. Nat Rev Mol Cell Biol 2009;10:165–77.
11. Holash J, Maisonpierre PC, Compton D, et al. Vessel cooption, regression, and growth in tumors mediated by angiopoietins and VEGF. Science 1999;284:1994–8.
12. Lobov IB, Brooks PC, Lang RA. Angiopoietin-2 displays VEGF-dependent modulation of capillary structure and endothelial cell survival *in vivo*. Proc Natl Acad Sci U S A 2002;99:11205–10.
13. Fiedler U, Reiss Y, Scharpfenecker M, et al. Angiopoietin-2 sensitizes endothelial cells to TNF-α and has a crucial role in the induction of inflammation. Nat Med 2006;12:235–9.
14. Imanishi Y, Hu B, Jarzynka MJ, et al. Angiopoietin-2 stimulates breast cancer metastasis through the α(5)β(1) integrin-mediated pathway. Cancer Res 2007;67:4254–63.
15. Tanaka S, Mori M, Sakamoto Y, Makuuchi M, Sugimachi K, Wands JR. Biologic significance of angiopoietin-2 expression in human hepatocellular carcinoma. J Clin Invest 1999;103:341–5.
16. Ahmad SA, Liu W, Jung YD, et al. Differential expression of angiopoietin-1 and angiopoietin-2 in colon carcinoma. A possible mechanism for the initiation of angiogenesis. Cancer 2001;92:1138–43.
17. Guo P, Imanishi Y, Cackowski FC, et al. Up-regulation of angiopoietin-2, matrix metalloprotease-2, membrane type 1 metalloprotease, and laminin 5 γ 2 correlates with the invasiveness of human glioma. Am J Pathol 2005;166:877–90.
18. Koga K, Todaka T, Morioka M, et al. Expression of angiopoietin-2 in human glioma cells and its role for angiogenesis. Cancer Res 2001; 61:6248–54.
19. Tanaka F, Ishikawa S, Yanagihara K, et al. Expression of angiopoietins and its clinical significance in non-small cell lung cancer. Cancer Res 2002;62:7124–9.
20. Helfrich I, Edler L, Sucker A, et al. Angiopoietin-2 levels are associated with disease progression in metastatic malignant melanoma. Clin Cancer Res 2009;15:1384–92.
21. Etoh T, Inoue H, Tanaka S, Barnard GF, Kitano S, Mori M. Angiopoietin-2 is related to tumor angiogenesis in gastric carcinoma: possible *in vivo* regulation via induction of proteases. Cancer Res 2001;61: 2145–53.
22. Hu B, Guo P, Fang Q, et al. Angiopoietin-2 induces human glioma invasion through the activation of matrix metalloprotease-2. Proc Natl Acad Sci U S A 2003;100:8904–9.
23. Yoshiji H, Kuriyama S, Noguchi R, et al. Angiopoietin 2 displays a vascular endothelial growth factor dependent synergistic effect in hepatocellular carcinoma development in mice. Gut 2005;54: 1768–75.
24. Machein MR, Knedla A, Knoth R, Wagner S, Neuschl E, Plate KH. Angiopoietin-1 promotes tumor angiogenesis in a rat glioma model. Am J Pathol 2004;165:1557–70.
25. Yu Q, Stamenkovic I. Angiopoietin-2 is implicated in the regulation of tumor angiogenesis. Am J Pathol 2001;158:563–70.
26. Nasarre P, Thomas M, Kruse K, et al. Host-derived angiopoietin-2 affects early stages of tumor development and vessel maturation but is dispensable for later stages of tumor growth. Cancer Res 2009;69:1324–33.
27. Fang HY, Hughes R, Murdoch C, et al. Hypoxia-inducible factors 1 and 2 are important transcriptional effectors in primary macrophages experiencing hypoxia. Blood 2009;114:844–59.
28. Klein RS, Lenzi M, Lim TH, Hotchkiss KA, Wilson P, Schwartz EL. Novel 6-substituted uracil analogs as inhibitors of the angiogenic actions of thymidine phosphorylase. Biochem Pharmacol 2001;62: 1257–63.
29. Lu H, Klein RS, Schwartz EL. Antiangiogenic and antitumor activity of 6-(2-aminoethyl)amino-5-chlorouracil, a novel small-molecule inhibitor of thymidine phosphorylase, in combination with the vascular endothelial growth factor-trap. Clin Cancer Res 2009;15:5136–44.
30. Urbich C, Rossig L, Kaluza D, et al. HDAC5 is a repressor of angiogenesis and determines the angiogenic gene expression pattern of endothelial cells. Blood 2009;113:5669–79.
31. Bureau W, Van Slyke P, Jones J, et al. Chronic systemic delivery of angiopoietin-2 reveals a possible independent angiogenic effect. Am J Physiol Heart Circ Physiol 2006;291:H948–56.
32. Reiss Y, Droste J, Heil M, et al. Angiopoietin-2 impairs revascularization after limb ischemia. Circ Res 2007;101:88–96.
33. Reiss Y, Knedla A, Tal AO, et al. Switching of vascular phenotypes within a murine breast cancer model induced by angiopoietin-2. J Pathol 2009;217:571–80.
34. Staton CA, Brown NJ, Rodgers GR, et al. Alphastatin, a 24-amino acid fragment of human fibrinogen, is a potent new inhibitor of activated endothelial cells *in vitro* and *in vivo*. Blood 2004;103:601–6.
35. Murdoch C, Muthana M, Coffelt SB, Lewis CE. The role of myeloid cells in the promotion of tumour angiogenesis. Nat Rev Cancer 2008; 8:618–31.
36. Du R, Lu KV, Petritsch C, et al. HIF1α induces the recruitment of bone marrow-derived vascular modulatory cells to regulate tumor angiogenesis and invasion. Cancer Cell 2008;13:206–20.
37. Bogdanovic E, Nguyen VP, Dumont DJ. Activation of Tie2 by angiopoietin-1 and angiopoietin-2 results in their release and receptor internalization. J Cell Sci 2006;119:3551–60.
38. Yuan HT, Khankin EV, Karumanchi SA, Parikh SM. Angiopoietin 2 is a partial agonist/antagonist of Tie2 signaling in the endothelium. Mol Cell Biol 2009;29:2011–22.
39. Hansen TM, Singh H, Tahir TA, Brindle NP. Effects of angiopoietins-1 and -2 on the receptor tyrosine kinase Tie2 are differentially regulated at the endothelial cell surface. Cell Signal 2010;22:527–32.
40. Marron MB, Singh H, Tahir TA, et al. Regulated proteolytic processing of Tie1 modulates ligand responsiveness of the receptor-tyrosine kinase Tie2. J Biol Chem 2007;282:30509–17.
41. Seegar TC, Eller B, Tzvetkova-Robev D, et al. Tie1-Tie2 interactions mediate functional differences between angiopoietin ligands. Mol Cell 2010;37:643–55.
42. Liekens S, Bronckaers A, Perez-Perez MJ, Balzarini J. Targeting platelet-derived endothelial cell growth factor/thymidine phosphorylase for cancer therapy. Biochem Pharmacol 2007;74:1555–67.
43. Engels K, Fox SB, Whitehouse RM, Gatter KC, Harris AL. Up-regulation of thymidine phosphorylase expression is associated with a discrete pattern of angiogenesis in ductal carcinomas *in situ* of the breast. J Pathol 1997;182:414–20.
44. Leek RD, Landers R, Fox SB, Ng F, Harris AL, Lewis CE. Association of tumour necrosis factor α and its receptors with thymidine phosphorylase expression in invasive breast carcinoma. Br J Cancer 1998;77:2246–51.
45. Mohamed MM, Sloane BF. Cysteine cathepsins: multifunctional enzymes in cancer. Nat Rev Cancer 2006;6:764–75.
46. Vasiljeva O, Papazoglou A, Kruger A, et al. Tumor cell-derived and macrophage-derived cathepsin B promotes progression and lung metastasis of mammary cancer. Cancer Res 2006;66:5242–50.
47. Gocheva V, Wang HW, Gadea BB, et al. IL-4 induces cathepsin protease activity in tumor-associated macrophages to promote cancer growth and invasion. Genes Dev 2010;24:241–55.
48. Mills CD, Kincaid K, Alt JM, Heilman MJ, Hill AM. M-1/M-2 macrophages and the Th1/Th2 paradigm. J Immunol 2000;164:6166–73.
49. Sica A, Larghi P, Mancino A, et al. Macrophage polarization in tumour progression. Semin Cancer Biol 2008;18:349–55.
50. Brown JL, Cao ZA, Pinzon-Ortiz M, et al. A human monoclonal anti-ANG2 antibody leads to broad antitumor activity in combination with VEGF inhibitors and chemotherapy agents in preclinical models. Mol Cancer Ther 2010;9:145–56.